Pavement Strains Induced by Spent-Fuel Transportation Trucks

RAJ SIDDHARTHAN, PETER E. SEBAALY, AND ZIA ZAFIR

Four types of vehicles are being considered for the transportation of spent-fuel casks to the high-level nuclear waste repository that is to be located in Yucca Mountain, Nevada. The use of a finite-layer moving-load model to compute the pavement strains is described. Pavement strains are required to compare the relative pavement damage caused by each of the spent-fuel trucks and to estimate the increased cost associated with the increase in maintenance and rehabilitation on pavements caused by the spent-fuel trucks. The strain response induced by the spent-fuel trucks for a site near Reno, Nevada, is reported. The asphalt concrete layer and the unbound materials are assumed viscoelastic and elastic, respectively. Pavement material propeties were deduced from falling-weight deflectometer testing. The study reveals that the strain response is affected strongly by the axle configuration and by the speed of the vehicle. Increased vehicle speed reduces the pavement strains substantially; longitudinal strains in the asphalt concrete layer decrease by as much as 33 percent when the speed of the vehicle increases from 30 to 60 km/hr. A substantial compressive strain component is also present when tandem and tridem axle loading are considered. The difference in contribution to pavement distress between the two legal-weight trucks and between the two overweight trucks is minimal. Laboratory fatigue and cyclic triaxial tests are being evaluated to compare the effects of legal-weight and overweight axle loading.

The Yucca Mountain area, located in the state of Nevada, is the only site being considered for storage of high-level nuclear spent fuel. Numerous studies are under way to assess the suitability of the site to store high-level nuclear spent fuel permanently. If the studies reveal no serious concerns, the repository is scheduled to receive spent-fuel elements from nuclear power plants early in the next century. A number of transportation modes are being appraised for transporting spent fuel from nuclear power plants to the site (*1*). One mode would be to use existing highways and specially designed trucks. Some of these trucks are overweight (heavier than the legal weight).

Both construction of the repository and transportation of spent fuel to the repository are expected to contribute to the deterioration of the existing highway pavements in Nevada. One objective of a study now under way at the University of Nevada, Reno, is to estimate the cost of maintaining pavements that might be affected by repository-related traffic to Yucca Mountain. In an attempt to quantify the cost, it is necessary to estimate the contribution of the repository-related traffic to the increase in maintenance and rehabilitation required to keep the pavement serviceable above some critical level.

Repository-related traffic's contribution to pavement distress or deterioration may be predicted using either empirical or mechanistic analyses (*2–4*). Empirical methods are based on AASHO road tests carried out in the 1960s. Mechanistic methods are based on pavement performance models that require traffic-induced pavement response (mainly strains) to predict pavement distress. The mechanistic approach, which uses fundamental pavement material properties, is considered a more rational approach and therefore has been adopted for the University of Nevada, Reno, study. Major modes of pavement distress are fatigue cracking, rutting, low-temperature cracking, roughness, and debonding. Widely used pavement distress models relate fatigue cracking to the horizontal tensile strain at the bottom of the asphalt concrete (AC) layer and the rutting to the vertical compressive strains at the top of the subgrade (*3–5*).

The distress or performance indicators just identified are often computed using static loading conditions, assuming either linear or nonlinear material characterization. Recently, Zafir (*6–8*) outlined an efficient finite-layer moving-load model that can predict pavement strains. The model accounts for the important dynamic effects of the moving load, such as inertia, damping (material and radiation), and wave reflection, and also presents the rate-dependent (viscoelastic material) properties. The AC layer is treated as viscoelastic, whereas the base and the subgrade are treated as linear elastic.

This paper describes the application of the aforementioned moving-load model to compute pavement strains caused by four types of trucks that are to be used in spent-fuel transportation. One approach to deducing viscoelastic material (required for the model) from falling-weight deflectometer (FWD) data is also presented.

EXISTING METHODS FOR PAVEMENT STRAINS

Moving traffic wheel loads exert dynamic forces on pavement; therefore, effects such as inertia, damping (material and radiation), and resonance become important. The response of deposits to moving surface pressure loading has been studied by a number of researchers. Excellent summaries of the description and applicability of the methods have been presented by Werkle and Waas (*9*) and Siddharthan et al. (*10*).

Widely used pavement response computer models such as ELSYM5 and BISAR are based on layered-elastic theory. These models assume static loading conditions and single or multiple circular loaded areas that are fixed in location. This means that moving-load (dynamic) effects and the rate-dependent material properties have been neglected.

Pavement engineers have known the importance of the dynamic loading caused by the moving load for some time (*3,4*). A recent extensive field testing program sponsored by FHWA at the Pennsylvania State University test track has clearly indicated the influ-

R. Siddharthan and P. Sebaaly, Department of Civil Engineering, University of Nevada, Reno, Nev. 89557. Z. Zafir, Geospectra, 3095 Richmond Parkway, Suite 213, Richmond, Calif. 94806.

ence of the dynamic nature of the wheel loading (*11,12*). In these studies two new pavement sections, representing a thin (0.15 m of AC over 0.2 m of crushed aggregate) and a thick (0.25 m of AC over 0.25 m of crushed aggregate) section were subjected to moving traffic loads.

The experimental program measured a wide range of pavement response histories, such as vertical deflection and longitudinal strain at the bottom of the AC layer under moving truck loads (Figure 1). Testing revealed that pavement responses are influenced strongly by the speed of a vehicle and by its wheel load acting on the pavement. There was a reduction of as much as 70 percent in the maximum tensile strain in the AC layer when the speed of the vehicle increased from 32 to 80 km/hr. Furthermore, the study clearly demonstrated that the strain history response is a result of the complex dynamic interaction between adjacent wheel loadings (in the case of tandem configuration), resulting in a substantial compressive strain (as much as 57 percent of the maximum tensile strain) component in the AC layer. Widely used computer models, such as ELSYM5 and BISAR, cannot predict the observed responses. A dynamic moving-load model that accounts for the rate-dependent material properties is required for this purpose.

The most recent study to predict the entire strain history response is based on the three-dimensional finite-element model (*13*). Sousa and his colleagues at the University of California, Berkeley, are also working on the development of a moving-load model that is also based on the finite-element method (J. B. Sousa, personal communication, 1993). The rate-dependent material properties can be accounted for in these models. To obtain accurate results, the finite-element techniques require a relatively fine finite-element mesh to accommodate large strain gradients, and the discretization should include a substantial lateral extent to model the moving load. There is no doubt that the computational effort associated with such an undertaking will be substantial.

Sousa et al. reported on an analytical model for computing pavement strains subjected to stationary circular loaded plates (*14,3*). They developed a computer model, SAPSI, to compute the response of a viscoelastic or elastic-layered system in the frequency domain. The input of the layer properties are Young's modulus, Poisson's ratio, and damping ratio as a function of the excitation frequency. The load-time history on the loaded areas varies as a function of

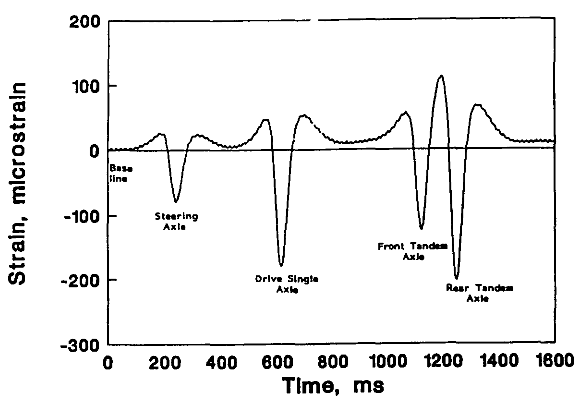

FIGURE 1 Measured longitudinal strain history in AC under moving semitrailer (*11,12*).

the velocity of the moving vehicle. Their approach is identical to one proposed by Sebaaly and Mamlouk (*15*).

However, these methods suffer from a major limitation in that they do not account for the true nature of the moving load. The assumption that a uniform pressure is present on the entire stationary loaded areas, even when the tire occupies only a part of the loaded area, is questionable. The assumption becomes more important, especially in the case of pavements, because the size of the loaded area and thickness of the AC layer are on the same order of magnitude.

BRIEF OUTLINE OF MOVING-LOAD MODEL

Zafir and Siddharthan (*6*) and Zafir et al. (*8*) reported on the formulation of a continuum-based, "finite layer" model to evaluate dynamic pavement strains subject to moving traffic load. Complex surface loadings, such as multiple loads and nonuniform tire-pavement interaction pressures, can be handled relatively easily because the method uses Fourier transform technique. The pavement layer system may be characterized as consisting of a number of viscoelastic or elastic horizontal layers (as many as necessary) with each layer characterized using a set of uniform properties. For viscoelastic materials, the Young's modulus, the Poisson's ratio, and the material damping vary as a function of excitation frequency. Laboratory tests to produce such relationships are available (*3,14*). Currently, the three-dimensional effects of the wheel loading are taken into account by the use of two special viscous boundaries (front and back) connected to the two-dimensional strip model shown in Figure 2. More details on the formulation of the model have been presented elsewhere (*6,8*).

GOVERNING EQUATIONS AND SOLUTION SCHEME

Figure 2 shows a horizontally layered pavement subjected to a moving traffic load at the surface. It depicts a modified plane strain model proposed by Lysmer and his coworkers (*16,17*). Forces acting on an element in the x direction are also shown. The element has a width B in the y direction equal to the width of the loading. The equations of motion at any point in the x and z directions can be written as follows:

$$\frac{\partial \sigma_x}{\partial x} + \frac{\partial \tau_{xz}}{\partial z} + \frac{2\rho V_s}{B}\frac{\partial u}{\partial t} = -\rho\frac{\partial^2 u}{\partial t^2} \tag{1}$$

$$\frac{\partial \sigma_z}{\partial z} + \frac{\partial \tau xz}{\partial z} + \frac{2\rho V_s}{B}\frac{\partial w}{\partial t} = -\rho\frac{\partial^2 w}{\partial t^2} \tag{2}$$

where

σ_x, σ_z = normal stresses (compressive) in the x and z directions, respectively;
τ_{xz} = shear stress;
ρ = mass density;
u, w = displacements in the x and z directions, respectively; and
V_s = shear wave velocity.

Because the surface load moves at a constant speed c and the pavement layer properties do not vary in the horizontal direction,

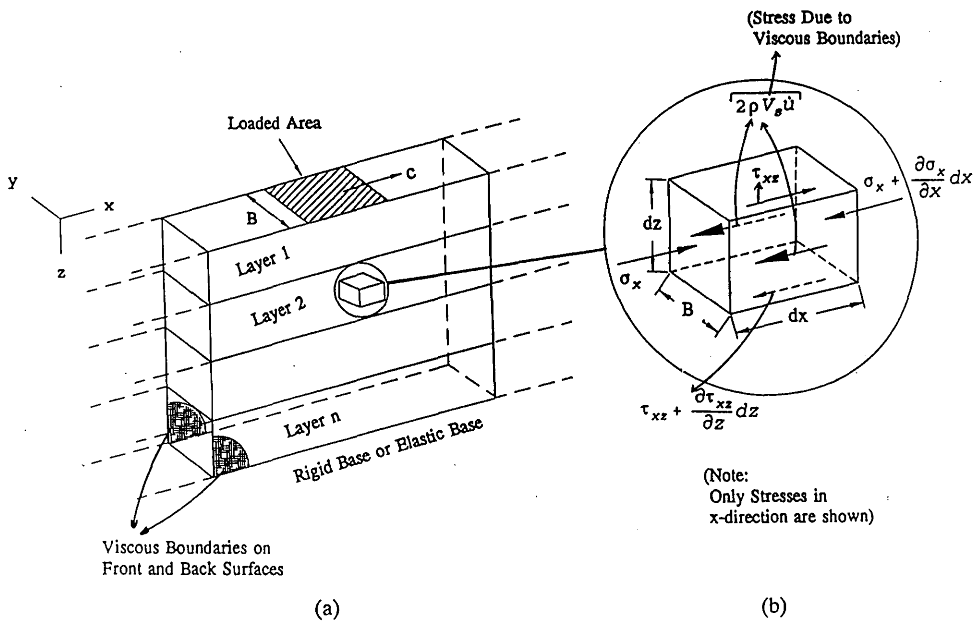

FIGURE 2 *(a)* **Rectangular load moving over layered medium;** *(b)* **stresses in an element.**

any response, say, for example, the displacement u using Fourier transform, can be written as

$$u = u(x - ct) = \text{Re} \sum_{n=0}^{N} U_n \exp[i\lambda_n(x - ct)] \tag{3}$$

where

U_n = variation in u with only z for the nth harmonic,
λ_n = wave number,
N = number of harmonics considered, and
$i = \sqrt{-1}$.

When responses are written in the form indicated in Equation 3, the derivatives with respect to x and t are simply

$$\frac{\partial u}{\partial x} = i\lambda_n u \qquad \frac{\partial u}{\partial t} = -i\lambda_n cu \tag{4}$$

After expansion of the stresses σ_x, σ_z, and τ_{xz} in terms of the displacements u and w, and subsequent use of the simplification presented in Equation 4, it is possible to derive the following equation for U_n from Equations 1 and 2:

$$\frac{d^4 U_n}{dz^4} + \left[-2\lambda_n^2 + \frac{\bar{\rho} c^2 \lambda_n^2 (3 - 4\nu)}{2(1 - \nu)G}\right] \frac{d^2 U_n}{dz^2} + \left[\lambda_n^4 - \frac{\bar{\rho} c^2 \lambda_n^4 (3 - 4\nu)}{2(1 - \nu)G} + \frac{\bar{\rho}^2 \lambda_n^4 c^4 (1 - 2\nu)}{2(1 - \nu)G^2}\right] U_n = 0 \tag{5}$$

where G is the shear modulus, ν is the Poisson's ratio, and $\bar{\rho}$ is given by

$$\bar{\rho} = \rho + \frac{2i\sqrt{G\rho}}{\lambda_n cB} \tag{6}$$

The solution to the fourth-order ordinary differential equation above can be obtained using the method of characteristics.

The boundary conditions are as follows: First, at the surface, σ_z equals the applied traffic load, and τ_{xz} equals zero. Second, at the bottom boundary, the displacements u and w are zero. At the interfaces between the layers, continuity relations in terms of displacement u, w, σ_z, and τ_{xz} need to be satisfied. Finally, the responses from all of the harmonics are algebraically added to get the complete response.

A computer code DYNPAVE has been developed incorporating the steps above. This program can handle any number of layers with any type of load distribution at the surface. The higher the number of layers, the larger the computational effort. At present, the code is capable of incorporating frequency-dependent properties for the AC layer at the same time that the base and subgrade are treated as linear-elastic layers. There is no practical limit to the number of horizontal layers that can be considered by the program. The material characterization used for the AC layer in the proposed study is presented subsequently. It was not necessary to consider all of the harmonics, because the contribution of the harmonics with large wave numbers (λ_n) is quite small. The computational effort associated with the proposed analysis can be reduced substantially by specifying a cutoff wave number above which the computation of the response is not required.

PAVEMENT STRAINS FOR SPENT-FUEL TRUCKS

Configuration of Spent-Fuel Trucks

Spent-fuel elements currently are stored near nuclear power plants, but they will need to be transported to the Yucca Mountain repository. Plans are to enclose the fuel elements in a cask and mount the cask on a flatbed truck. A proposed cask-trailer system is presented in Figure 3. A detailed study has identified several types of trucks, both typical and atypical, that might possibly be

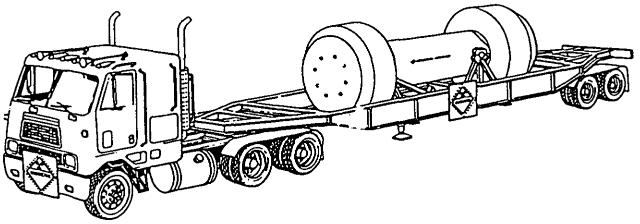

FIGURE 3 Typical spent-fuel truck and cask.

used in the spent-fuel transportation to the repository (*18*). The four types of vehicles under consideration are

- Existing legal-weight truck (LWT1),
- Future legal-weight truck (LWT2),
- Existing overweight truck (OWT1), and
- Future overweight truck (OWT2).

Table 1 shows the payload, gross vehicle weight, axle configuration, and axle load distribution for each vehicle. The overweight trucks use a tridem axle, whereas the legal-weight trucks use a tandem axle. It may be noted that if overweight trucks are used, there will be fewer trips to the repository site. On the other hand, overweight trucks' speed on state routes and through mountainous terrain will be slower.

Site and Material Characterization

The University of Nevada, Reno, and the Nevada Department of Transportation collected extensive FWD data for at least 4 years and during all four seasons on a variety of pavements located within the state. The data base consists of FWD measurements taken at 27 sites at 15.2-m intervals covering each test section, 305 m long. FWD testing using the Dynatest FWD model 8000 was carried out at four load levels, varying from 27 kN to as much as 90 kN (*19*).

Deflection basins obtained in the FWD tests were used with the MODULUS program to backcalculate layer moduli (*20*). Note that when using the MODULUS program the thickness of the subgrade layer is not required because the variable is treated as an additional unknown along with layer modulus values. The program is much more efficient than other backcalculation programs and yields reasonable results. Results from the program have been used to construct a resilient-modulus data base for all sites and all four seasons (*19,21*).

From this extensive data base, only the results corresponding to Site 24, which is located near Reno, Nevada, have been selected for the site-specific study reported in this paper. Pavement layer thicknesses obtained from coring and the average pavement layer resilient modulus values for summer were extracted from the data base and are shown in Figure 4 (*19,21*).

It may be noted that the proposed dynamic pavement response model is capable of handling viscoelastic characterization for the layers. Because only the AC layer exhibits strong frequency-dependent behavior, the viscoelastic layer characterization is used for the AC layer, and the base and the subgrade layers are assumed to be elastic. For the AC layer, the frequency-dependent resilient modulus must be deduced from the resilient moduli (elastic) backcalculated from FWD tests. A procedure adopted to achieve this is presented below.

Figure 5 indicates the load pulses applied during FWD testing. Two pulses are presented that have been normalized so that the shapes of the pulses can be seen clearly. The normalized Fourier transforms obtained for these pulses are represented in Figure 6. It is clear from Figures 5 and 6 that the dominant frequency range associated with the pulses is quite wide (up to 30 Hz). In other words, the backcalculated AC resilient modulus from FWD testing is, in fact, a representative value for this wide range of dominant frequencies.

Sousa and Monismith (*22*) studied the effects of different parameters on the resilient modulus of AC. The AC samples were tested under three different temperatures, 11, 25, and 40°C, and

TABLE 1 Cask and Vehicle Types and Weight Distribution

Vehicle Type	Loaded Cask Weight, kN	Gross Vehicle Weight (GVW), kN	Axle Configuration and Loads, kN
LWT1: Legal Weight	200.0	331.4	Single-Tandem-Tandem 44.5 - 144.6 - 142.3
LWT2: Future Legal Weight	224.6	351.4	Single-Tandem-Tandem 48.9 - 151.2 - 151.2
OWT1: Current overweight	349.6	493.7	Single-Tridem-Tridem 53.4 - 209.1 - 231.3
OWT2: Future Overweight	355.8	516.0	Single-Tridem-Tridem 48.9 - 226.8 - 240.2

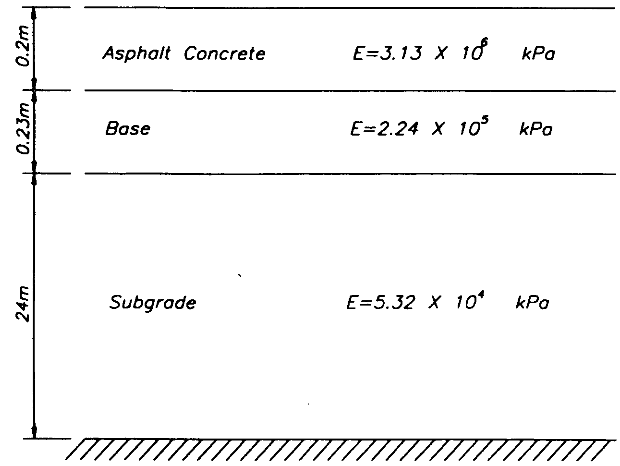

FIGURE 4 Pavement layer configuration at Site 24.

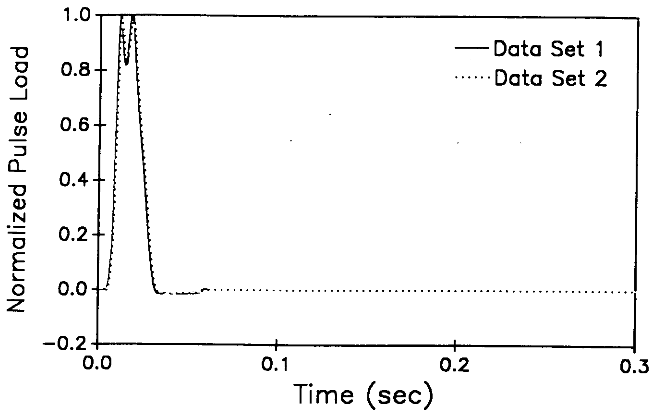

FIGURE 5 Normalized FWD pulses.

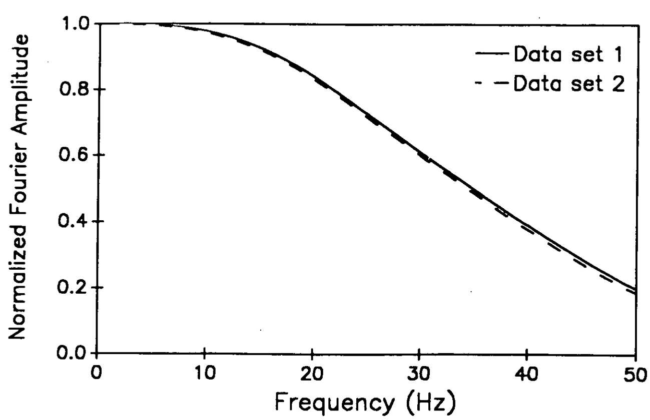

FIGURE 6 Normalized Fourier amplitude of FWD pulses.

were subjected to sinusoidal cyclic axial and torsional loading with varying frequencies. They found that for AC the amplitude of the dynamic complex Young's modulus $|E^*|$ is a function of temperature and frequency of the loading (Figure 7). Figure 7 illustrates that the dynamic Young's modulus for AC increases with an increase in frequency and decreases with an increase in temperature.

The steps employed to arrive at the frequency-dependent AC modulus can be summarized as follows:

1. Assume that the curves, $|E^*|$ versus frequency (f), given in Figure 7 are master curves. This means that the variation in $\log|E^*|$ in summer (T = 25°C) at Site 24 will vary linearly with $\log(f)$ as shown in Figure 8. Therefore, if E_o^*, which is the value of $|E^*|$ at f = 1 Hz, is known, the entire variation of E^* with frequency can be defined. Then an equation for $|E_n^*|$ at 25°C and at a frequency f_n (Figure 7) is given by the following:

$$\log|E_n^*| = \log(E_o^*) + 0.165 \log(f_n) \qquad (7)$$

2. Assume a value for E_o^*, and compute the axial strain ϵ_f as

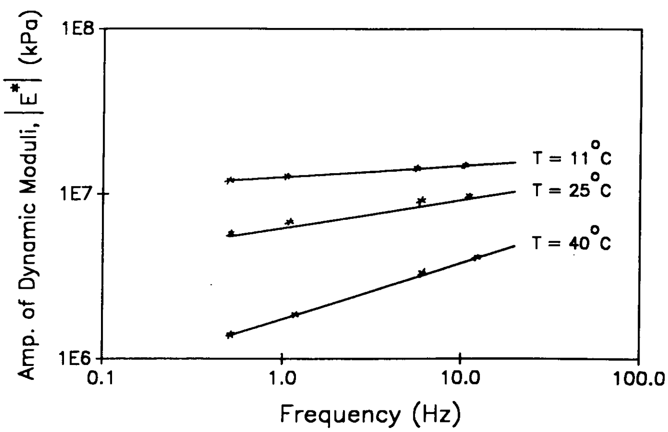

FIGURE 7 Variation of AC resilient modulus with frequency (23).

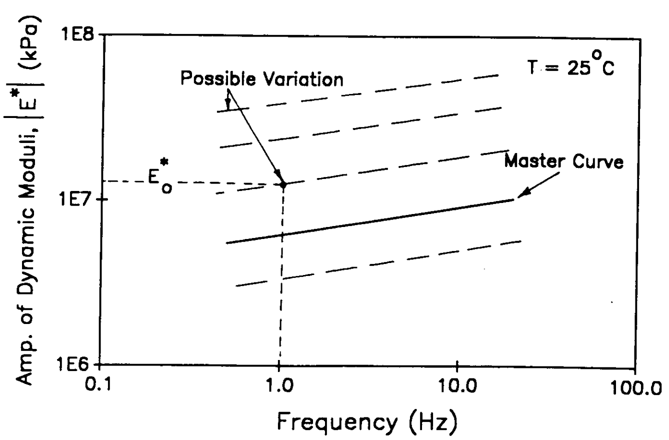

FIGURE 8 Curve fitting to obtain $|E^*|$ variation.

$$\epsilon_f = \sum_{n=0}^{N} \frac{P(t)}{|E_n^*|} = \sum_{n=0}^{N} \frac{p_n}{|E_n^*|} \tag{8}$$

where $P(t)$ and p_n are the pulse loading (Figure 5) and the corresponding Fourier amplitude.

3. Compute the axial strain ϵ_{fwd} that corresponds to the resilient modulus derived from FWD analysis as

$$\epsilon_{fwd} = \frac{1}{E_{AC}} \tag{9}$$

where E_{AC} is the resilient modulus given for AC by the FWD backcalculation. Note that unit pressure was used in the computations of ϵ_f and ϵ_{fwd}.

4. If the difference between ϵ_{fwd} and ϵ_f is not within an acceptable limit (say, 5μ), repeat Steps 2 through 4 with a new E_o^* until convergence is achieved.

5. Once the convergence has been reached, the value of E_o^* substituted into Equation 7 gives the variation of $|E^*|$ with the frequency for the AC layer at any site.

Convergence was reached for Site 24 (during summer) for $E_o^* = 8.3 \times 10^5$ kPa. Other material properties, such as a dynamic Poisson's ratio and the material damping, are assumed to be those reported by Sousa and Monismith (*22*).

Results of Pavement Strains

In pavement design, the contact area is determined by dividing the load on each tire by the contact pressure. In the literature the tire-pavement contact area often has been approximated by a rectangle ($0.4\,L \times 0.6\,L$) and two semicircles with a radius of $0.3L$ as shown in Figure 9(a), in which L is the total length of the loaded area. L can be obtained following Yoder and Witczak (*2*) or Huang (*3*) as follows:

$$L = \sqrt{\frac{A_c}{0.5227}} \tag{10}$$

where A_c is the contact area. Because the proposed approach can handle only a rectangular loaded area, one must arrive at an equivalent rectangular loaded area. The proposed equivalent rectangular area is indicated by dotted lines in Figure 9(a). The equivalent loaded area was obtained by selecting the length of the rectangle, such that the area of the rectangle equals A_c. Dual tires may be modeled by combining the two rectangular loaded areas as indicated in Figure 9(b). The tire pressure in all of the results reported here was assumed to be 861 kPa.

Although the program DYNPAVE can compute strain, stress, displacement, and acceleration at any point, only longitudinal strain response at the bottom of the AC layer is reported in this paper. A typical computed time history response of longitudinal strain for a tridem axle traveling at a speed of 60 km/hr is shown in Figure 10. Each tire in the axle was assumed to carry 19.3 kN, giving a total of 232 kN for the axle. There are three tensile axial strain peaks representing the three loaded axles. The maximum tensile and compressive strains are 435 and 168μ. Two observations similar to those made by Sebaaly et al. (*11,12*) in the field can be made: (a) the strain response has both tensile and a substantial compressive strain, and (b) the strain response is a result of complex interaction between adjacent wheels.

Figure 11 shows the maximum tensile and compressive AC strain and the vertical compressive subgrade strain induced by all four vehicles traveling at 60 km/hr. The tensile AC strains vary between 434 and 439μ, whereas the compressive AC strains vary between 168 and 175μ. The small variation in AC strains induced

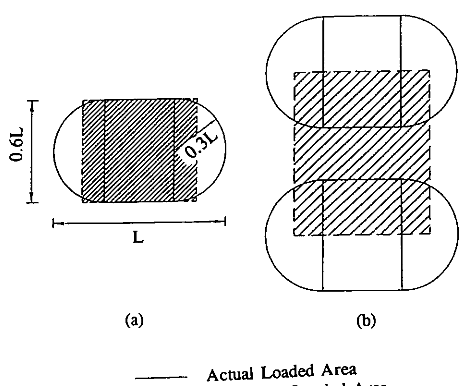

FIGURE 9 Approximate loaded areas for single and dual tires.

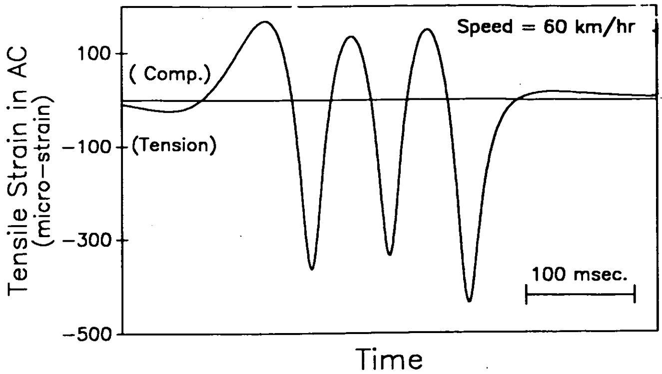

FIGURE 10 Computed tensile strain history induced in AC by tridem axle.

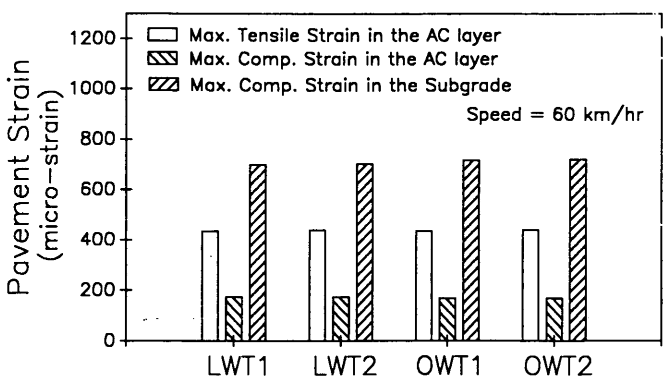

FIGURE 11 Dynamic pavement strains induced by spent-fuel trucks.

by the vehicles can be attributed to similar maximum load and tire values for the vehicles (see Table 1). The maximum compressive strain in the AC is as much as 40 percent of the maximum tensile strain. Note that, even though the maximum AC strains (tensile and compressive) may not be substantially different between tridem and tandem axle configurations, three and two strain pulses are caused by these configurations, respectively. The influence of the difference in the number of pulses on pavement damage can be quite important, and it can be evaluated readily in the laboratory using fatigue beam tests.

Vertical compressive strain in the subgrade varies between 698 and 720μ for all the vehicles. Higher strains are induced by overweight trucks. Unlike the AC strains, the axle configuration has a somewhat higher influence on the magnitude of the subgrade strain. However, because of the limited number of spent-fuel casks to be transported, the increase in the magnitude of the subgrade strain associated with the overweight trucks is not considered critical. However, given the different characteristics of the pulses generated by the tandem and tridem vehicles, their effect on the permanent deformation of the subgrade may be dissimilar.

The effect of vehicle speed on maximum tensile strain induced in the AC layer is illustrated in Figure 12. Reduction in strain is quite substantial in all cases (i.e., a decrease from 538 to 361μ—a reduction of 33 percent—when the speed of the LWT1 vehicle increased from 30 to 90 km/hr).

On the basis of the results of the DYNPAVE analyses presented in Figures 11 and 12, it can be concluded that axle configuration and vehicle speed are the most critical factors. Various vehicles considered here apply strain pulses with similar maximum amplitude yet different characteristics. Vehicle speed, however, is highly significant in determining the level of strain induced on the pavement. Therefore, in order to clearly identify the effects of various types of trucks on pavement performance, the influence of these factors must be considered.

It is evident from the results presented that the difference in contribution to pavement damage by the two legal-weight trucks, LWT1 and LWT2, is insignificant. This is also true for the overweight trucks, OWT1 and OWT2. It was pointed out earlier that the overweight trucks with heavier loads and tridem axle configuration will be traveling more slowly than the legal-weight trucks. Furthermore, it is customary for state departments of transportation to assign a speed limit to overweight trucks. On the other hand, the overweight trucks will carry heavier loads, which will reduce the number of trips they must make to the repository. Therefore, comparison of the effects of the overweight and legal-weight trucks is basically a choice between lower speed, more pulses, and fewer trips and higher speed, fewer pulses, and more trips. An effort to quantify these differences is under way at the University of Nevada, Reno.

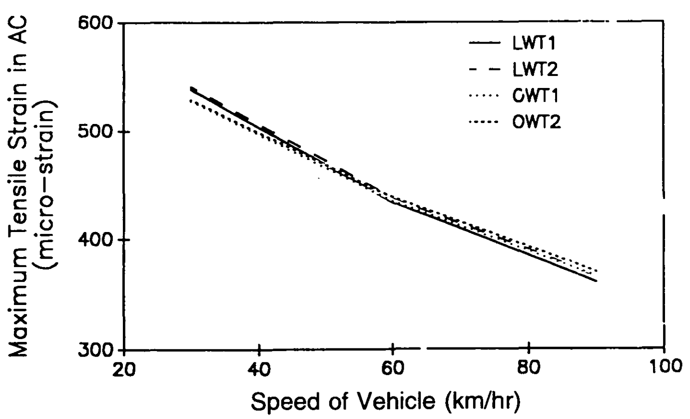

FIGURE 12 Variation of maximum tensile strain in AC with speed of vehicle.

SUMMARY AND CONCLUSIONS

Four types of vehicles were identified as vehicles that may be used to transport spent-fuel casks to Yucca Mountain in Nevada. The increase in traffic from spent-fuel trucks traveling to the repository will accelerate pavement deterioration in the state. One of the major goals of a study under way at the University of Nevada, Reno, is an estimation of the cost associated with the additional maintenance and rehabilitation of roads serving repository traffic.

To use mechanistic methods to evaluate pavement distress, strains induced on the pavement must be measured. This paper describes the use of a newly developed "finite-layer" moving-load model to compute pavement strains. In the model, a pavement layer system may be characterized as viscoelastic or as having elastic layers. The related computer program, DYNPAVE, can handle any number of layers with any type of load distribution at the surface.

A site near Reno, Nevada, was tested, and the response of the longitudinal strain in the AC layer and the vertical compressive strain in the subgrade caused by all four types of spent-fuel trucks were reported. The frequency-dependent material properties (viscoelastic) of the AC layer were deduced from the Fourier transform of the FWD load pulse, based on the assumption that the amplitude of the resilient modulus varies linearly with the logarithm of the frequency. Dynamic tests on triaxial samples support this assumption. The base and the subgrade were considered elastic, and their resilient modulus values were deduced from the data base of backcalculated moduli derived from FWD measurements.

The AC strain history results are similar to those reported by Sebaaly et al. (*11,12*), who measured AC strains under a moving semitrailer. The results reported in this paper indicate that (*a*) the strain response is a result of a complex interaction between adjacent wheel loads, (*b*) a substantial compressive strain component is present (as much as 40 percent of the tensile strain), and (*c*) the strain response is affected strongly by the speed of the vehicle.

The maximum tensile strain in the AC layer induced by the four trucks traveling at 60 km/hr varies between 434 and 439μ. The study reveals that the magnitudes of two important pavement strains (tensile strain in the AC and compressive strain in the subgrade) are similar for legal-weight vehicles considered in the study. Therefore, similar pavement deterioration may be expected from legal-weight trucks. Overweight trucks indicated the identical result. On the other hand, the characteristics of the strain pulses generated by the overweight trucks will be quite different from those generated by the legal-weight trucks because different axle configurations are used in the vehicles. Laboratory fatigue tests on AC beams and cyclic tests on subgrade soils are being considered to quantify the deterioration associated with the strain histories generated by tridem and tandem axle loading.

An increase in vehicle speed reduced the longitudinal strain in the AC layer by as much as 33 percent when the speed increased from 30 to 60 km/hr. This result has serious implications. Legal-weight trucks may travel faster, and thus induce smaller strains. However, they would need to make more trips to the repository to deliver the same number of spent-fuel tanks. Research to quantify these factors and to evaluate trucks different effects on pavement deterioration is under way.

REFERENCES

1. Office of Civilian Radioactive Waste Management. *Department of Energy Section 175 Report.* Report DOE/RW-0205. U.S. Department of Energy, Dec. 1988.
2. Yoder, E. J. and M. W. Witczak. *Principles of Pavement Design,* 2nd ed., John Wiley and Sons, Inc., New York, 1975.
3. Monismith, C. L. Analytically Based Asphalt Pavement Design and Rehabilitation: Theory to Practice, 1962–1992. In *Transportation Research Record 1354,* TRB, National Research Council, Washington, D.C., 1992, pp. 5–26.
4. Huang, Y. H. *Pavement Analysis and Design.* Prentice Hall, Englewood Cliffs, N.J., 1993.
5. *Thickness Design: Asphalt Pavements for Highways and Streets.* Manual Series No. 1 (MS-1). Asphalt Institute, College Park, Md., Feb. 1991.
6. Zafir, Z. and R. Siddharthan. Dynamic Response of Elastic Layered Medium to Moving Loads, *Proc., 33rd AIAA/ASME Conference on Structures, Structural Dynamics, and Materials,* Dallas, Tex. Vol. 3, April 1992, pp. 1549–1557.
7. Zafir, Z. *Response of Layered Media to Moving Loads.* Ph.D. dissertation. Civil Engineering Department, University of Nevada, Reno, 1993.
8. Zafir, Z., R. Siddharthan, and P. Sebaaly. Dynamic Pavement Strain Histories from Moving Traffic Load. *Journal of Transportation Engineering,* ASCE, Oct. 1993.
9. Werkle, H. and G. Waas. Analysis of Ground Motion Caused by Propagating Air Pressure Waves. *Journal of Soil Dynamics and Earthquake Engineering,* Vol. 6, 1987, pp. 196–202.
10. Siddharthan, R., Z. Zafir, and G. M. Norris. Moving Load Response of Layered Soil I: Formulation. *Journal of Engineering Mechanics,* ASCE, Vol. 119, No. 10, Oct. 1993, pp. 2052–2071.
11. Sebaaly, P. E., N. Tabatabaee, B. T. Kulakowski, and T. Scullion. *Instrumentation for Flexible Pavements; Field Performance of Selected Sensors,* Final Report Vol. I and II. Report FHWA-RD-91-094. FHWA, U.S. Department of Transportation, Sept. 1991.
12. Sebaaly, P. E., and N. Tabatabaee. Influence of Vehicle Speed on Dynamic Loads and Pavement Response. In *Transportation Research Record 1410,* TRB, National Research Council, Washington, D.C., 1993, pp. 107–114.
13. Huhtala, M., and J. Pihlajamäki. New Concepts on Load Equivalency Measurements. *Proc., 7th International Conference on Asphalt Pavements,* Nottingham, England, 1992, pp. 194–208.
14. Sousa, J. B., J. Lysmer, S. S. Chen, and C. L. Monismith. Effects of Dynamic Loads on Performance of Asphalt Concrete Pavements. In *Transportation Research Record 1207,* TRB, National Research Council, Washington, D.C., 1988, pp. 145–168.
15. Sebaaly, P. E., and M. S. Mamlouk. Prediction of Pavement Response to Actual Traffic Loading. Presented at 66th Annual Meeting of the Transportation Research Board, Washington, D.C., Jan. 1989.
16. Hwang, R. N., J. Lysmer, and E. Berger. A Simplified Three-Dimensional Soil-Structure Interaction Study. *Proc., 2nd Specialty Conference on Structural Design of Nuclear Plant Facilities,* New Orleans, La., Vol. I-A, Dec. 1975, pp. 786–808.
17. Lysmer, J., T. Udaka, C. F. Tsai, and H. B. Seed. FLUSH: *A Computer Program for Approximate 3-D Analysis of Soil-Structure Interaction Problems.* Report EERC 75-30. University of California, Berkeley, Nov. 1975.
18. *Overweight Truck Shipments to Nuclear Waste Repositories: Legal, Political, Administrative and Operational Considerations.* Technical Report BMI/OTSP-01. Battelle Memorial Institute, Columbus, Ohio, March 1986.
19. Sebaaly, P. E., R. Siddharthan, M. Javaregowda, and S. Srikantiah. *Mechanistic Overlay Design Procedure for the State of Nevada.* Report 410-4. Nevada Department of Transportation, Carson City, June 1992.
20. Lytton, R. L., F. P. Germann, Y. J. Chou, and S. M. Stoffels. *NCHRP Report 327: Determining Asphaltic Concrete Pavement Structural Properties by Nondestructive Testing.* TRB, National Research Council, Washington, D.C., June 1990, 105 pp.
21. Siddharthan, R., P. E. Sebaaly, and M. Javaregowda. Influence of Statistical Variation in Falling Weight Deflectometers on Pavement Analysis. In *Transportation Research Record 1377,* TRB, National Research Council, Washington, D.C., 1992, pp. 57–66.
22. Sousa, J. B. and C. L. Monismith. Dynamic Response of Paving Materials. In *Transportation Research Record 1136,* TRB, National Research Council, Washington, D.C., 1987, pp. 57–68.

Publication of this paper sponsored by Committee on Strength and Deformation Characteristics of Pavement Sections.